AGU PUBLICATIONS

Geophysical Research Letters

On the suitability of North Brazil Current transport estimates for monitoring basin-scale AMOC changes

Siren Rühs[1], Klaus Getzlaff[1], Jonathan V. Durgadoo[1], Arne Biastoch[1], and Claus W. Böning[1]

[1]GEOMAR Helmholtz-Zentrum für Ozeanforschung Kiel, Kiel, Germany

Abstract The North Brazil Current (NBC) constitutes a bottleneck for the mean northward return flow of the Atlantic Meridional Overturning Circulation (AMOC) in the tropical South Atlantic. Previous studies suggested a link between interannual to multidecadal NBC and AMOC transport variability and proposed to use NBC observations as an index for the AMOC. Here we use a set of hindcast, sensitivity, and perturbation experiments performed within a hierarchy of ocean general circulation models to show that decadal to multidecadal buoyancy-forced changes in the basin-scale AMOC transport indeed manifest themselves in the NBC. The relation is, however, masked by a strong interannual to decadal wind-driven gyre variability of the NBC. While questioning the NBC transport as a "direct" index for the AMOC, the results support its potential merit for an AMOC monitoring system, provided that the wind-driven circulation variability is properly accounted for.

1. Introduction

The Atlantic Meridional Overturning Circulation (AMOC) is a key feature of Earth's climate [e.g., *Lozier*, 2012]. It is closely related to the oceanic meridional heat transport [*Ferrari and Ferreira*, 2011; *Msadek et al.*, 2013] and sequestration of climate-relevant chemical compounds such as carbon dioxide [*Pérez et al.*, 2013]. It fundamentally contributes to the regulation of regional and global climate by influencing surface air temperatures, precipitation, and sea level pattern [*Knight et al.*, 2005; *Zhang and Delworth*, 2006; *Lorbacher et al.*, 2010]. The prospect of a dwindling AMOC strength in the next decades as projected by climate studies [*Intergovernmental Panel on Climate Change* (*IPCC*), 2013] has motivated extensive efforts to investigate the variability of the AMOC, including several monitoring projects [*Srokosz and Bryden*, 2015]. The most prominent observing system is the RAPID-MOCHA trans-basin array deployed at 26.5°N since 2004 [*Cunningham et al.*, 2007; *McCarthy et al.*, 2015]. Studies building on its evolving transport record have greatly enhanced the knowledge of intraseasonal to interannual AMOC variability in the subtropical North Atlantic [*Srokosz and Bryden*, 2015]. They further stimulated the establishment, continuation, and expansion of transport arrays at other latitudes in the Atlantic, e.g., MOVE at 16°N [*Send et al.*, 2011], SAMBA at 34.5°S [*Meinen et al.*, 2013; *Ansorge et al.*, 2014], and OSNAP at 53°N (http://www.o-snap.org/). Given the resources needed to establish and maintain such extensive arrays, it is of interest to identify more easily accessible indices of AMOC trends and variability, which could supplement the basin-scale monitoring.

In the tropical Atlantic, the North Brazil Current (NBC) constitutes a bottleneck for the interhemispheric mean flow of the upper limb of the AMOC. The NBC originates off the Brazilian continental shelf, where the southern branch of the South Equatorial Current bifurcates [*da Silveira et al.*, 1994]. It merges all upper and intermediate layer northward flow of the tropical South Atlantic, yielding observed mean transports exceeding 20 Sv (Sverdrup, 1 Sv = 10^6 m^3/s) between 11°S and 5°S, with a subsurface current core at about 200 m depth [*Stramma et al.*, 1995; *Johns et al.*, 1998; *Schott et al.*, 2005]. After crossing the equator, the NBC transport diminishes, because it seasonally retroflects into the zonal equatorial current system [*Johns et al.*, 1998]. At the retroflection at 5°–8°N, anticyclonic eddies are shed, whose northwestward migration contributes to a mean tropical to subtropical cross-gyre transport and represents a major part of the upper limb of the AMOC in this regime [*Barnier et al.*, 2001; *Johns et al.*, 2003; *Jochumsen et al.*, 2010]. A comprehensive collection of NBC measurements in the western tropical South Atlantic is provided by *Schott et al.* [2005], including results of repeated shipboard sections at 5°S and 11°S and of a moored array deployed near 11°S between 2000 and 2004. In July 2013, the moored array has been redeployed and is anticipated to be maintained [*Hummels et al.*, 2015].

Previous model studies suggested a close link between NBC and AMOC variability on interannual to decadal time scales [e.g., *Hüttl and Böning*, 2006; *Chang et al.*, 2008; *Rabe et al.*, 2008], hinting at the possible use of NBC transport estimates as an index for the AMOC variability. More recently, *Zhang et al.* [2011] inferred a geostrophic NBC transport time series based on four decades (1956–1999) of hydrographic observations near the western boundary of the tropical South Atlantic. This revealed decadal NBC transport changes with a range of about 7 Sv in broad coherence with variations of AMOC related climate indices, such as the Atlantic Multidecadal Oscillation [*Knight et al.*, 2005] and the Labrador Sea deep convection [*Curry et al.*, 1998].

Open questions concern the mechanisms responsible for NBC variability on interannual to multidecadal time scales. As a western boundary current, the NBC is not only part of the basin-scale AMOC but also of the wind-driven equatorial gyre circulation and contributes to the shallow overturning of subtropical-tropical cells. Thus, NBC variability can arise from remote impacts on the AMOC, e.g., changes in subarctic deep water formation [*Yeager and Danabasoglu*, 2014], or in Agulhas leakage [*Biastoch et al.*, 2008a; *Rühs et al.*, 2013], as well as from wind-driven variability in the tropical-subtropical ocean circulation [*Hüttl and Böning*, 2006]. Despite a growing understanding of the principal forcing mechanisms and ongoing observational measurement campaigns, the origin of NBC transport variability on interannual and longer time scales has not been fully explained.

In this study, we use a set of model experiments performed within a hierarchy of ocean general circulation models (OGCMs) to explore the respective role of the basin-scale buoyancy-forced AMOC variability versus more local wind-driven circulation changes on the NBC transport variability. The following questions are addressed: (1) How robust are ocean hindcasts of meridional transports in the tropical South Atlantic? (2) What is the nature of interannual to decadal NBC variability; do decadal NBC changes reflect changes in the basin-scale AMOC? (3) Would possible future multidecadal trends in the AMOC manifest themselves in the NBC transport?

2. Data and Methods

2.1. Hindcast, Sensitivity, and Perturbation Experiments Performed With OGCMs

We use monthly mean output between 1960 and 2007 of a set of hindcast, sensitivity, and perturbation experiments performed with four global ocean/sea-ice OGCM configurations, all formulated with the Nucleus for European Modeling of the Ocean (version 3.1) [*Madec*, 2008], and developed within the DRAKKAR framework [*The DRAKKAR Group*, 2014].

A hindcast performed with ORCA025 [*Barnier et al.*, 2006] serves as a reference experiment (denoted REF). ORCA025 uses a tripolar grid, with a nominal horizontal resolution of 1/4°, and 46 vertical levels with increasing grid spacing from 6 m near the surface to 250 m at depth. Interannually varying air-sea fluxes were used to force the model, using the methodology and atmospheric forcing products from 1948 to 2007 of the Coordinated Ocean-ice Reference Experiments (CORE, version 2) [*Large and Yeager*, 2008; *Griffies et al.*, 2009]. Air-sea freshwater fluxes were complemented by climatological monthly river runoff. Turbulent air-sea fluxes were calculated during the model integration through bulk formulae. The model was spun up from rest for 30 years (1978–2007); to account for possible spin-up transients in the velocity fields, only results after 1960 are considered in the analysis.

To assess the robustness of the results, additional hindcast configurations were utilized, which follow the same model set up and forcing as REF, but vary in their horizontal resolutions from 1/2° to 1/20°. They differ in their representations, e.g., of the details of the current field in the western tropical Atlantic and in remote regions potentially important for the mean state and variability of the AMOC. The configurations are the following: (1) ORCA05, a global non-eddying configuration with nominal 1/2° grid spacing [*Behrens et al.*, 2013]; (2) INALT01, a global 1/2° configuration refined in the South Atlantic and western Indian Ocean via two-way nesting [*Debreu and Blayo*, 2008], including a higher resolution in the NBC, as well as an improved representation of the extended Agulhas region [*Durgadoo et al.*, 2013]; and (3) VIKING20, a global 1/4° configuration with 1/20° refinement in the North Atlantic (30°–85°N), included here because it shows an improved representation of the subarctic deep water formation and corresponding mean AMOC patterns [*Behrens*, 2013] and thus contributes to assessing the robustness of the results.
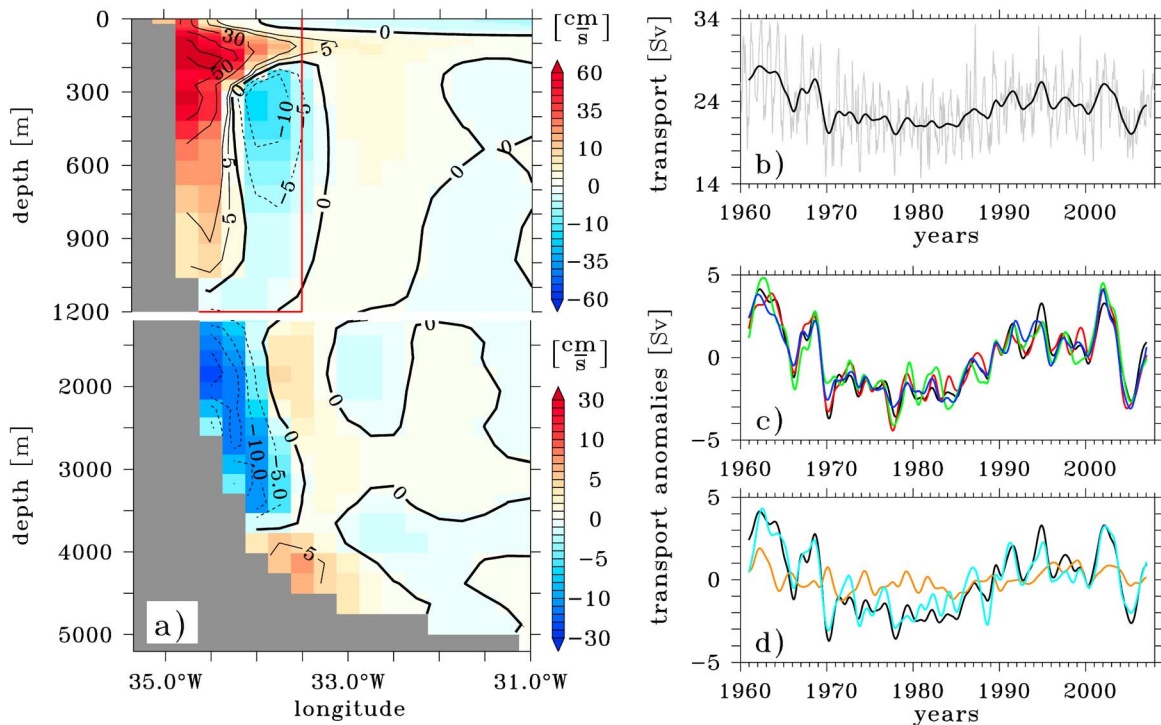
Figure 1. NBC at 6°S in the western tropical Atlantic: (a) Mean meridional flow (contours and color shading) for REF; the NBC transport is defined by the integrated positive meridional (= northward) velocities between the coast and 33.5°W, and 0–1200 m depth (red box). (b) Monthly (thin) and interannual (thick) NBC transport time series for REF. Interannual NBC transport anomalies for (c) REF (black), ORCA05 (dark blue), VIKING20 (red), and INALT01 (green), and (d) REF (black), BUOY (orange), and WIND (light blue).

To further explore the mechanisms of variability and to distinguish wind-driven from buoyancy-driven variability on interannual to longer time scales, we included results of two sensitivity experiments, referred to as WIND and BUOY, respectively. These were performed with the REF configuration but with modified forcing. We followed the approach by *Biastoch et al.* [2008b], by combining wind stress from repeated year wind forcing with interannually varying heat and freshwater forcing for BUOY, and interannually varying wind stress forcing with repeated year heat and freshwater forcing for WIND.

A final pair of experiments was devised to assess the manifestation of multidecadal AMOC trends in the NBC. Building on the REF experiment, two cases with gradually decreasing (MOC−) and increasing (MOC+) AMOC strength were generated by artificially increasing and decreasing the prescribed precipitation in the subarctic Atlantic, respectively (cf. *Behrens et al.* [2013] for the sensitivity of the AMOC to small perturbations in the subarctic freshwater fluxes). Further information about the ocean models and experiments can be found at the GEOMAR homepage (http://www.geomar.de/en/research/fb1/fb1-tm/ocean-models) and in Tables S1 and S2.

2.2. Calculation of NBC Transport and AMOC Strength Time Series

As recently shown, despite latitudinal differences in the mean NBC transport, its interannual variability is mainly coherent between 11°S and 5°S [*Hummels et al.*, 2015]. Here we focus on the NBC transport variability and its relation to the AMOC at 6°S, since this is the latitude already referred to by *Zhang et al.* [2011], and there exist historical and new observational estimates of the NBC transport [*Schott et al.*, 2005; *Hummels et al.*, 2015]. In agreement with former studies [*Schott et al.*, 2005; *Rabe et al.*, 2008; *Zhang et al.*, 2011], we define the NBC transport by the integrated positive meridional velocities between the coast and 33.5°W, and 0–1200 m depth (Figure 1a). Only the near-coast northward transport of the NBC is considered, because it is the most practical definition (easy to measure), and well correlated with more complex estimates including farther offshore recirculation cells [*Hummels et al.*, 2015]. Also, we repeated parts of the analysis for a NBC definition including its first recirculation, with no essential changes in the results (Text S1 and Figures S1 and S2).
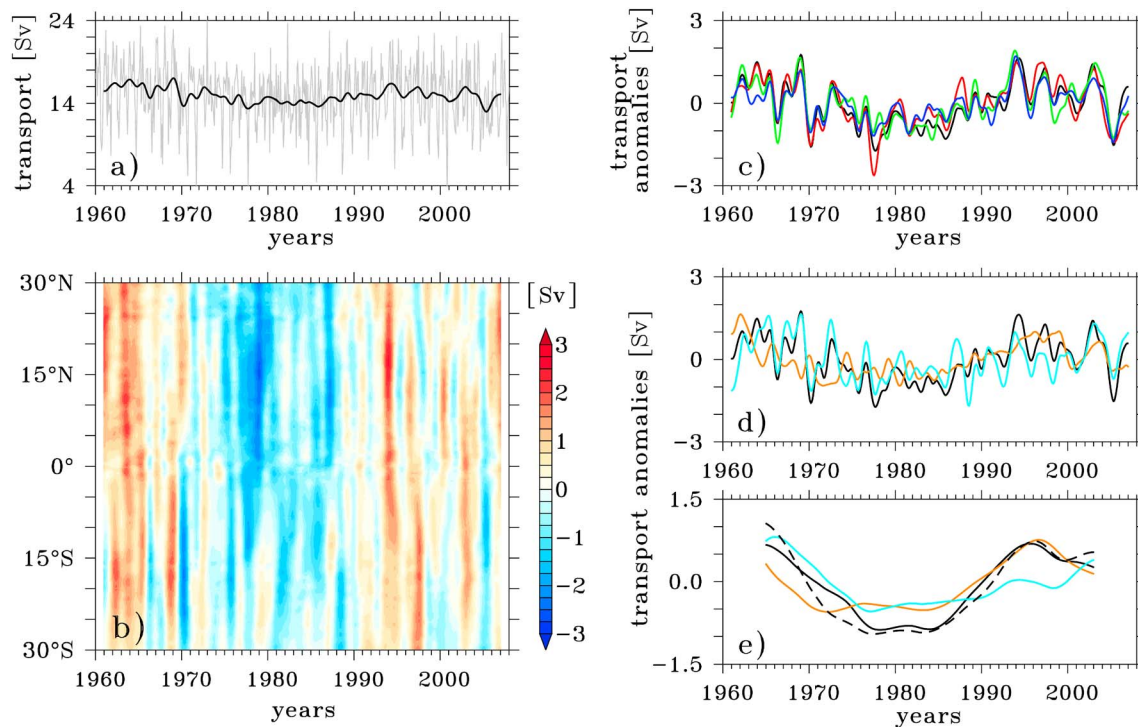
Figure 2. (a) Monthly (thin) and interannual (thick) AMOC strength time series at 6°S and (b) Hovmöller plot of interannual AMOC strength anomalies for REF. Interannual AMOC strength anomalies at 6°S for (c) REF (black), ORCA05 (dark blue), VIKING20 (red), and INALT01 (green), and (d) REF (black), BUOY (orange), and WIND (light blue). (e) As in Figure 2d but for decadal AMOC variability and with additional curve representing a linear superposition of BUOY and WIND (black dashed).

The strength of the AMOC is defined at each latitude as the maximum of the meridional overturning stream function below 500 m depth; in the tropical to subtropical Atlantic, the maximum is located around 1000 m depth.

For the comparisons of the hindcast and sensitivity experiments, NBC and AMOC transport time series were detrended, since AMOC simulations are prone to include nonnegligible spurious drifts (Table S1 and Text S2), which are rather to be attributed to the model configuration than to the forcing [*Behrens et al.,* 2013]. To assess the mechanisms of variability, we follow previous studies [e.g., *Biastoch et al.,* 2008b; *Yeager and Danabasoglu*, 2014] and distinguish decadal variability (119 month low-pass filtered) from interannual variability (23 month low-pass filtered). The effect of long-term trends is separately investigated by the use of the perturbation experiments MOC+ and MOC−.

3. Results

3.1. Nature of Interannual to Decadal NBC Transport Variability

Figure 1b shows the monthly time series of the NBC transport at 6°S obtained from REF. The simulated long-term (1960–2007) mean transport of 23.6 ± 3.7 Sv (uncertainties are given in terms of 1 standard deviation σ) lies at the lower end of the observed range of 26.5 ± 3.7 Sv reported by *Schott et al.* [2005]. If only considering the period 1990–2004, when measurements were taken, REF agrees better with observations (Table S2).

However, in accordance with previous studies [*Barnier et al.,* 2001], mean transports are found to be sensitive to the model configuration. The suite of hindcast simulations yield mean NBC transports ranging from 21.5 to 27.8 Sv (Table S1). Despite these differences in the mean transport, Figure 1c illustrates that the magnitude ($1.9 \leq \sigma \leq 2.0$ Sv, Table S1) and evolution of NBC transport anomalies on interannual and longer time scales are strikingly similar in all simulations. They show a relatively strong NBC transport in the 1960s, followed by a weak period between 1970 and 1985, and a strengthened NBC in the 1990s. These simulated decadal changes are also overall consistent in magnitude and phase with the NBC transport changes reconstructed from observations by *Zhang et al.* [2011], suggesting that the simulations can provide a meaningful basis to investigate the mechanisms of NBC variability (for a detailed comparison, see *Hummels et al.* [2015]).

A first aspect pertinent to the nature of the interannual to decadal NBC variability is the robustness of the signal. The small model-model differences—including the 1/10° configuration with well-resolved mesoscale processes (INALT01)—suggest a primarily deterministic character of the transport variability, with an only minor impact of intrinsic (stochastic) variability. Figure 1d further reveals that most interannual to decadal NBC variability inherent in the hindcasts is also captured by the WIND sensitivity experiment. In contrast, there is less similarity between the hindcasts and BUOY. This is also reflected in the standard deviations of the interannual NBC anomalies ($\sigma_{REF} = 1.9$, $\sigma_{WIND} = 1.8$, and $\sigma_{BUOY} = 0.6$ Sv).

The finding of a major contribution of wind-driven circulation variability to the interannual to decadal NBC transport changes during the last five decades appears to be in some contrast to former interpretations of the decadal NBC signal as the manifestation of basin-scale AMOC changes, associated with buoyancy-forced variations in the formation of Labrador Sea Water [*Zhang et al.*, 2011]. In the next section, we show that AMOC and NBC indeed varied in phase. Yet we further discuss why the in-phase relation cannot necessarily be interpreted as a direct imprint of the basin-scale buoyancy-driven AMOC variability on the NBC.

3.2. Imprint of Decadal Basin-Scale AMOC Changes on the NBC

Figure 2a shows the simulated (REF) monthly mean time series of the AMOC strength at 6°S in the Atlantic, with a mean transport of 14.9 ± 3.7 Sv (1960–2007). Lack of observational records precludes quantitative model verifications at this latitude, but some useful assessments are possible at 26°N.

The simulated (REF) mean AMOC strength at 26°N of 15.3 ± 2.3 Sv lies at the lower end of the observed range of 17.0 ± 3.5 Sv obtained from the RAPID program (based on 2004–2014 monthly means). However, as for the NBC, the mean AMOC strength differs between the members of the model hierarchy (ranging from 13.9 Sv to 21.2 Sv at 26°N, Table S1), mainly associated with model-model differences in the representation of water mass characteristics and transformation processes in the subpolar North Atlantic [cf. *Danabasoglu et al.*, 2014]. Despite these strong differences in the mean AMOC, its variability is again similar among all hindcast experiments. The monthly mean transport time series exhibit a pronounced variability, with a dominant seasonal cycle and standard deviations between 2.3 and 2.8 Sv at 26°N, which roughly compares to the 3.5 Sv in the RAPID record. This high-frequency variability is strongest in the tropics, where it partially masks the lower frequency variability (Figure S3). Yet low-pass filtering yields a robust signal on interannual to decadal time scales, with only little model-model differences.

Concerning the interannual AMOC variability at 6°S, the hindcast simulations (Figure 2c) show a good agreement with the time series obtained from WIND (Figure 2d), indicating a substantial impact of wind-driven circulation changes also on the AMOC variability. The interannual variability is superimposed onto a weaker decadal signal, which, as for the NBC, is characterized by a relatively strong transport in the 1960s, followed by a weak phase between 1970 and 1985, and a generally strengthened AMOC in the 1990s. A similar signature of decadal AMOC changes is present in the whole Atlantic basin, whereas the year-to-year variability is less meridionally coherent and often hemispherically or even locally confined (Figures 2b and S4). Thus, as already pointed out by *Johnson and Marshall* [2004], the year-to-year variability of the AMOC is strongly dependent on the regional forcing and cannot necessarily be associated with basin-scale changes in the strength of the overturning.

In the following, we focus on decadal AMOC variability at 6°S (Figure 2e): On this time scale, the AMOC variability can be regarded as a superposition of decadal wind-driven circulation changes and buoyancy-driven variability. Consistent with the analysis of forcing contributions provided by *Yeager and Danabasoglu* [2014], the wind-driven contribution to the AMOC variability is not negligible at this latitude. Interestingly, the buoyancy-driven and the wind-driven components vary approximately in phase over the simulation period and equally contribute to the weakening of the AMOC observed in the first decades, whereas the more recent increase seems to be dominated by buoyancy-driven changes.

As already noted, the simulated AMOC transport shows a similar decadal evolution as the NBC. Yet a direct comparison of the decadal variability in the NBC and AMOC time series at 6°S (Figure 3a) illustrates that the decadal NBC variability is approximately twice as large in magnitude. When only considering the buoyancy-driven part of the decadal AMOC and NBC variability (Figure 3b), a good agreement in phase and amplitude can be detected. This is in line with former studies, which showed that remote changes in the AMOC, e.g., caused by buoyancy-driven changes in the Labrador Sea deep convection, evoke a
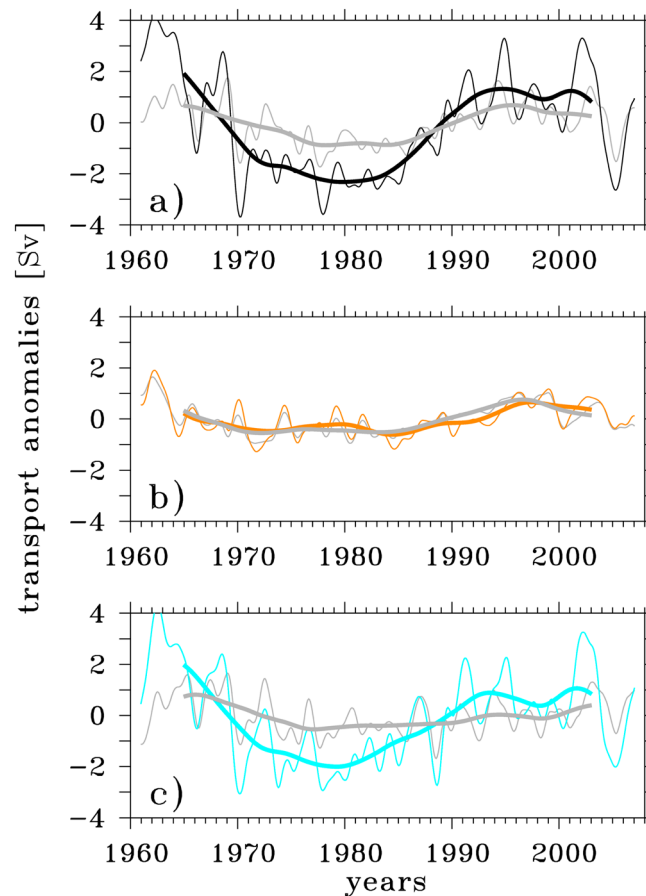
Figure 3. Relation between NBC and AMOC variability at 6°S: Interannual (thin) and decadal (thick) NBC transport (colored) and AMOC strength (grey) anomalies in (a) REF, (b) BUOY, and (c) WIND.

corresponding but attenuated AMOC signal in the tropics, concentrated at the western boundary [*Zhang*, 2010; *Hüttl and Böning*, 2006]. However, the wind-driven components of the decadal AMOC and NBC variability (Figure 3c) show less agreement. In particular, the magnitude of the wind-driven NBC variability ($\sigma = 1.1$ Sv) is larger than that of the wind-driven AMOC variability ($\sigma = 0.4$ Sv). This can only be explained by the manifestation of horizontal gyre circulation changes in the NBC, which do not impact the strength of the overturning.

In summary, the results of the hindcast and sensitivity experiments suggest that the low-frequency changes in NBC transport during the last decades do not directly reflect decadal variability of the basin-scale AMOC. The NBC variability captures the AMOC variability but has an additional even larger contribution from decadal wind-driven changes of the horizontal gyre circulation.

3.3. Manifestation of Possible Future Multidecadal AMOC Trends in the NBC

Finally, we examine the suitability of sustained NBC transport measurements for monitoring possible future trends in the AMOC, e.g., a gradual weakening of the basin-scale AMOC due to anthropogenic warming or freshening of surface waters in the subarctic Atlantic [*IPCC*, 2013]. A way to study the imprint of such AMOC trends is provided by the two perturbation experiments MOC+ and MOC−. The forcing for the individual realizations is identical to the one used for REF, apart from the perturbation in the subarctic freshwater fluxes. Thus, the transport time series include the same remote and local forcing contributions characterizing the reference case, including the strong wind-driven variability. The effect of the remotely induced AMOC trends is isolated by subtracting the transport time series of one perturbation experiment from the other.

Figure 4a shows the temporal evolution of the AMOC strength for both experiments, Figure 4b the respective evolution of the NBC transport at 6°S. The interannual to decadal variability as discussed above is still reflected in the time series and again more pronounced in the NBC than in the AMOC. However, the dominant new features are positive and negative multidecadal trends in the AMOC strength in MOC+ and MOC−, respectively, with corresponding trends in the NBC time series (Table S1). Note that the AMOC trends represent basin-scale changes–they are inherent in the South Atlantic at 6°S as well as in the subtropical Atlantic at 26°N (Figure 4a).

The evolution of the difference in the AMOC and NBC transports between the two perturbation experiments (Figure 4c) shows a striking correspondence: The NBC at 6°S nearly perfectly traces the evolution of the AMOC. Figures 4d and 4e further show that the changes in the NBC are meridionally coherent: The mean (2000–2007) transport density of MOC+ is increased compared to MOC− over the whole latitudinal extent of the NBC. We conclude that multidecadal trends in the basin-scale AMOC manifest themselves in the NBC.
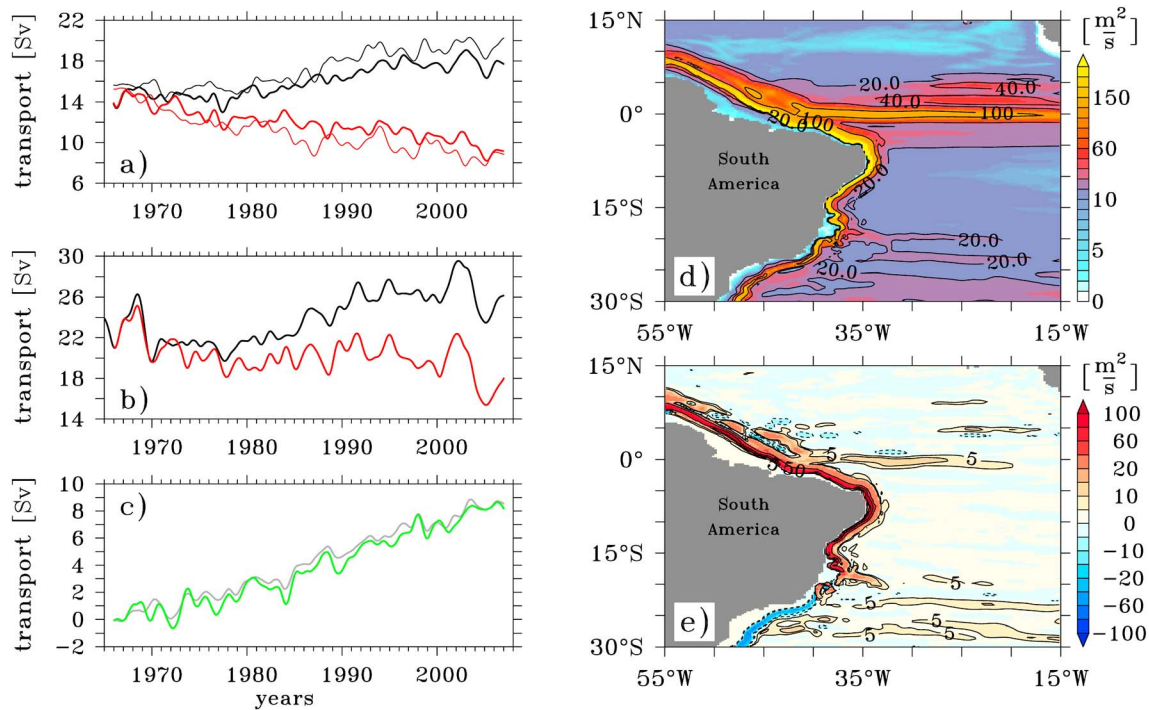
Figure 4. Perturbation experiments: Interannual time series of (a) AMOC strength at 6°S (thick) and 26°N (thin), and (b) NBC transport at 6°S for MOC− (red) and MOC+ (black). (c) Difference in AMOC strength (blue) and NBC (green) between the experiments (MOC+ minus MOC−). (d) Mean (2000–2007) upper ocean circulation pattern in the western subtropical-tropical Atlantic visualized by the transport density (current speed integrated over 0–1200 m depth) in MOC+. (e) Mean (2000–2007) difference (MOC+ minus MOC−) in the transport density.

4. Conclusions

Our analysis shows that (1) NBC transport estimates from different model configurations yield a robust interannual to decadal variability for the past decades, indicating a rather deterministic character of NBC transport variability; (2) the NBC variability of the past decades has been mainly wind-driven; the basin-scale decadal variability of the AMOC is captured in the NBC but has been dominated by a strong wind-driven gyre variability on interannual to decadal time scales; and (3) possible future multidecadal AMOC trends manifest themselves in the NBC and could be derived from its transport time series if interannual to decadal wind-driven gyre changes are properly accounted for.

In contrast to former studies [e.g., *Zhang et al.,* 2011], the skill of the NBC transport as a *direct* index for the basin-scale AMOC strength appears to be limited. Surprisingly, during the last decades, the basin-scale AMOC and wind-driven gyre circulation varied approximately in phase. Thus, the good correspondence of the observed and simulated NBC transport changes with the conceived [*Zhang et al.,* 2011] and simulated (this study) decadal changes of the basin-scale AMOC mainly reflects an in-phase variation of the different forcing components. The question that remains is whether this represents a mere coincidence of the last decades or constitutes a more general feature of the atmospheric forcing patterns of the Atlantic Ocean. As long as the in-phase relation between the different forcing components cannot be sufficiently explained and, in particular, is not been shown to be stable in time, NBC transport measurements on their own cannot be used to reliably infer decadal basin-scale AMOC changes.

However, our results also suggest that the NBC transport *corrected* for its wind-driven gyre component could possibly serve as an index for basin-scale AMOC variability on decadal to multidecadal time scales. At least for the last decades, removing an estimate of the wind-driven component given by the Sverdrup relation from the NBC variability already leads to an improved correspondence between NBC and AMOC transport anomalies (not shown). The correspondence could possibly be further enhanced by considering a more comprehensive model of the wind-driven circulation. For an explicit formulation of such an index, which would only require boundary current measurements and a record of near-surface wind stress, further work is required.

With these considerations, we conclude that boundary current arrays in the western tropical South Atlantic, such as the mooring array investigated in *Hummels et al.* [2015], could serve as a cost-effective complement to long-term trans-basin arrays at higher latitudes.

References

Ansorge, I. J., et al. (2014), Basin-wide oceanographic array bridges the South Atlantic, *Eos Trans. AGU*, *95*(6), 53–54, doi:10.1002/2014EO060001.

Barnier, B., T. Reynaud, A. Beckmann, C. Böning, J.-M. Molines, S. Barnard, and Y. Jia (2001), On the seasonal variability and eddies in the North Brazil Current: Insights from model intercomparison experiments, *Prog. Oceanogr.*, *48*(2–3), 195–230, doi:10.1016/S0079-6611(01)00005-2.

Barnier, B., et al. (2006), Impact of partial steps and momentum advection schemes in a global ocean circulation model at eddy-permitting resolution, *Ocean Dyn.*, *56*, 543–567, doi:10.1007/s10236-006-0082-1.

Behrens, E. (2013), The oceanic response to Greenland melting: The effect of increasing model resolution, PhD thesis, Fac. of Math. and Nat. Sci., Christian-Albrechts-Univ. zu Kiel, Kiel, Germany.

Behrens, E., A. Biastoch, and C. W. Böning (2013), Spurious AMOC trends in global ocean sea-ice models related to subarctic freshwater forcing, *Ocean Modell.*, *69*, 39–49, doi:10.1016/j.ocemod.2013.05.004.

Biastoch, A., C. W. Böning, and J. R. E. Lutjeharms (2008a), Agulhas leakage dynamics affects decadal variability in Atlantic overturning circulation, *Nature*, *456*(7221), 489–492, doi:10.1038/nature07426.

Biastoch, A., C. W. Böning, J. Getzlaff, J.-M. Molines, and G. Madec (2008b), Causes of interannual-decadal variability in the meridional overturning circulation of the midlatitude North Atlantic Ocean, *J. Clim.*, *21*(24), 6599–6615, doi:10.1175/2008JCLI2404.1.

Chang, P., R. Zhang, W. Hazeleger, C. Wen, X. Wan, L. Ji, R. J. Haarsma, W.-P. Breugem, and H. Seidel (2008), Oceanic link between abrupt changes in the North Atlantic Ocean and the African monsoon, *Nat. Geosci.*, *1*(7), 444–448, doi:10.1038/ngeo218.

Cunningham, S. A., et al. (2007), Temporal variability of the Atlantic Meridional Overturning Circulation at 26.5°N, *Science*, *317*(5840), 935–938, doi:10.1126/science.1141304.

Curry, R. G., M. S. McCartney, and T. M. Joyce (1998), Oceanic transport of subpolar climate signals to mid-depth subtropical waters, *Nature*, *391*(6667), 575–577, doi:10.1038/35356.

Danabasoglu, G., et al. (2014), North Atlantic simulations in Coordinated Ocean-ice Reference Experiments phase II (CORE-II). Part I: Mean states, *Ocean Modell.*, *73*, 76–107, doi:10.1016/j.ocemod.2013.10.005.

da Silveira, I. C. A., L. B. de Miranda, and W. S. Brown (1994), On the origins of the North Brazil Current, *J. Geophys. Res.*, *99*(C11), 22,501–22,512, doi:10.1029/94JC01776.

Debreu, L., and E. Blayo (2008), Two-way embedding algorithms: A review, *Ocean Dyn.*, *58*, 415–428, doi:10.1007/s10236-008-0150-9.

Durgadoo, J. V., B. R. Loveday, C. J. C. Reason, P. Penven, and A. Biastoch (2013), Agulhas leakage predominantly responds to the Southern Hemisphere westerlies, *J. Phys. Oceanogr.*, *43*(10), 2113–2131, doi:10.1175/JPO-D-13-047.1.

Ferrari, R., and D. Ferreira (2011), What processes drive the ocean heat transport?, *Ocean Modell.*, *38*(3–4), 171–186, doi:10.1016/j.ocemod.2011.02.013.

Griffies, S., et al. (2009), Coordinated Ocean-ice Reference Experiments (COREs), *Ocean Modell.*, *26*, 1–46, doi:10.1016/j.ocemod.2008.08.007.

Hummels, R., P. Brandt, M. Dengler, J. Fischer, M. Araujo, D. Veleda, and J. V. Durgadoo (2015), Interannual to decadal changes in the western boundary circulation in the Atlantic at 11°S, *Geophys. Res. Lett.*, *42*, doi:10.1002/2015GL065254, in press.

Hüttl, S., and C. W. Böning (2006), Mechanisms of decadal variability in the shallow subtropical-tropical circulation of the Atlantic Ocean: A model study, *J. Geophys. Res.*, *111*, C07011, doi:10.1029/2005JC003414.

Intergovernmental Panel on Climate Change (IPCC) (2013), *Climate Change 2013: The Physical Science Basis. Contribution of Working Group I to the Fifth Assessment Report of the Intergovernmental Panel on Climate Change*, Cambridge Univ. Press, Cambridge, U. K., and New York.

Jochumsen, K., M. Rhein, S. Hüttl-Kabus, and C. W. Böning (2010), On the propagation and decay of North Brazil Current rings, *J. Geophys. Res.*, *115*, C10004, doi:10.1029/2009JC006042.

Johns, W., T. Lee, R. C. Beardsley, J. Candela, R. Limeburner, and B. Castro (1998), Annual cycle and variability of the North Brazil Current, *J. Phys. Oceanogr.*, *28*, 103–128, doi:10.1175/1520-0485(1998)028<0103:ACAVOT>2.0.CO;2.

Johns, W., R. Zantopp, and G. Goni (2003), Cross-gyre transport by North Brazil Current rings, *Elsevier Oceanogr. Ser.*, *68*, 411–441.

Johnson, H. L., and D. P. Marshall (2004), Global teleconnections of meridional overturning circulation anomalies, *J. Phys. Oceanogr.*, *34*, 1702–1722, doi:10.1175/1520-0485(2004)034<1702:GTOMOC>2.0.CO;2.

Knight, J. R., R. J. Allan, C. K. Folland, M. Vellinga, and M. E. Mann (2005), A signature of persistent natural thermohaline circulation cycles in observed climate, *Geophys. Res. Lett.*, *32*, L20708, doi:10.1029/2005GL024233.

Large, W. G., and S. G. Yeager (2008), The global climatology of an interannually varying air-sea flux data set, *Clim. Dyn.*, *33*, 341–364, doi:10.1007/s00382-008-0441-3.

Lorbacher, K., J. Dengg, C. W. Böning, and A. Biastoch (2010), Regional patterns of sea level change related to interannual variability and multidecadal trends in the Atlantic meridional overturning circulation, *J. Clim.*, *23*(15), 4243–4254, doi:10.1175/2010JCLI3341.1.

Lozier, M. S. (2012), Overturning in the North Atlantic, *Annu. Rev. Mar. Sci.*, *4*, 291–315, doi:10.1146/annurev-marine-120710-100740.

Madec, G. (2008), NEMO ocean engine, Note du Pole de modelisation, No. 27. Inst. Pierre-Simon Laplace (IPSL), France.

McCarthy, G. D., et al. (2015), Measuring the Atlantic Meridional Overturning Circulation at 26°N, *Prog. Oceanogr.*, *130*, 91–111, doi:10.1175/JCLI-D-13-00052.1.

Meinen, C. S., S. Speich, R. C. Perez, S. Dong, A. R. Piola, S. L. Garzoli, M. O. Baringer, S. Gladyshev, and E. J. D. Campos (2013), Temporal variability of the meridional overturning circulation at 34.5°S: Results from two pilot boundary arrays in the South Atlantic, *J. Geophys. Res. Oceans*, *118*, 6461–6478, doi:10.1002/2013JC009228.

Msadek, R., W. E. Johns, S. G. Yeager, G. Danabasoglu, T. L. Delworth, and A. Rosati (2013), The Atlantic meridional heat transport at 26.5°N and its relationship with the MOC in the RAPID Array and the GFDL and NCAR coupled models, *J. Clim.*, *26*(12), 4335–4356, doi:10.1175/JCLI-D-12-00081.1.

Pérez, F. F., H. Mercier, M. Vázquez-Rodríguez, P. Lherminier, A. Velo, P. C. Pardo, G. Rosón, F. Aida, and A. Ríos (2013), Atlantic Ocean CO_2 uptake reduced by weakening of the meridional overturning circulation, *Nat. Geosci.*, *6*(2), 146–152, doi:10.1038/ngeo1680.

Rabe, B., F. A. Schott, and A. Köhl (2008), Mean circulation and variability of the tropical Atlantic during 1952–2001 in the GECCO assimilation fields, *J. Phys. Oceanogr.*, *38*(1), 177–192, doi:10.1175/2007JPO3541.1.

Rühs, S., J. V. Durgadoo, E. Behrens, and A. Biastoch (2013), Advective time scales and pathways of Agulhas leakage, *Geophys. Res. Lett.*, *40*, 3997–4000, doi:10.1002/grl.50782.

Schott, F. A., M. Dengler, R. Zantopp, L. Stramma, J. Fischer, and P. Brandt (2005), The shallow and deep western boundary circulation of the South Atlantic at 5°–11°S, *J. Phys. Oceanogr.*, *35*, 2031–2053, doi:10.1175/JPO2813.1.

Send, U., M. Lankhorst, and T. Kanzow (2011), Observation of decadal change in the Atlantic Meridional Overturning Circulation using 10 years of continuous transport data, *Geophys. Res. Lett.*, *38*, L24606, doi:10.1029/2011GL049801.

Srokosz, M., and H. L. Bryden (2015), Observing the Atlantic Meridional Overturning Circulation yields a decade of inevitable surprises, *Science*, *348*(6241), 1255575, doi:10.1126/science.1255575.

Stramma, L., J. Fischer, and J. Reppin (1995), The North Brazil Undercurrent, *Deep Sea Res., Part I*, *42*(5), 773–795, doi:10.1016/0967-0637(95)00014-W.

The DRAKKAR Group (2014), DRAKKAR: Developing high resolution ocean components for European Earth system models, *CLIVAR Exch.*, *65*, 18–21.

Yeager, S., and G. Danabasoglu (2014), The origins of late-twentieth-century variations in the large-scale North Atlantic Circulation, *J. Clim.*, *27*(9), 3222–3247, doi:10.1175/JCLI-D-13-00125.1.

Zhang, D., R. Msadek, M. J. McPhaden, and T. Delworth (2011), Decadal variability of the North Brazil Current and its connection to the Atlantic meridional overturning circulation, *J. Geophys. Res.*, *116*, C04012, doi:10.1029/2010JC006812.

Zhang, R. (2010), Latitudinal dependence of Atlantic Meridional Overturning Circulation (AMOC) variations, *Geophys. Res. Lett.*, *37*, L16703, doi:10.1029/2010GL044474.

Zhang, R., and T. L. Delworth (2006), Impact of Atlantic multidecadal oscillations on India/Sahel rainfall and Atlantic hurricanes, *Geophys. Res. Lett.*, *33*, L17712, doi:10.1029/2006GL026267.